The identification of Fe^{2+} in the $M(4)$ site of calcic amphiboles

DON S. GOLDMAN AND GEORGE R. ROSSMAN

Division of Geological and Planetary Sciences
California Institute of Technology
Pasadena, California 91125

Abstract

Evidence is presented for the occurrence of Fe^{2+} in the predominantly Ca-filled $M(4)$ site of calcic amphiboles. Absorption bands in the electronic spectra at 1030 nm in β and at 2470 in α provide a sensitive means for identifying Fe^{2+} in this site. The large ϵ value for the 1030 band, the large energy separation between both bands, and the similarity to the spectra of Fe^{2+} in large, highly distorted coordination sites in other minerals provide the basis for the $M(4)$ site assignment. The energy splittings and polarization anisotropy of these bands are analyzed using a point-charge model based on C_{2v} symmetry. Spectral data indicate that the Fe^{2+} content in the $M(4)$ site varies significantly among the calcic amphiboles.

Introduction

Little is known about the Fe^{2+} content of the $M(4)$ site of calcic amphiboles. $M(4)$ Fe^{2+} has been difficult to identify because calcium generally occupies 85–95 percent of this site (Leake, 1968); therefore, only a small percentage of the total iron in most samples can occupy the $M(4)$ site. Hence, it is difficult to analyze for $M(4)$ Fe^{2+} in the complex Mössbauer spectra, and to detect small quantities of Fe^{2+} in a predominantly Ca-filled $M(4)$ site by crystallographic analysis. The purpose of this paper is to identify Fe^{2+} in the $M(4)$ site with electronic absorption spectra and to show that this technique is sensitive to small concentrations of Fe^{2+} in this site.

The electronic absorption spectra of the calcic amphiboles consist of a superposition of absorption bands that arise from ferrous iron in several sites of different coordination geometries. Amphiboles contain three sites $M(1)$, $M(2)$, and $M(3)$ that more closely resemble regular octahedra than the fourth site, $M(4)$, which is highly distorted from octahedral geometry. Fe^{2+} in the $M(4)$ site of calcic amphiboles has not been previously identified in absorption spectra. Burns (1970) presented absorption spectra of two actinolites, $Ca_2(Mg,Fe)_5Si_8O_{22}(OH)_2$, in the 350–1500 nm region in which all Fe^{2+} features were attributed to Fe^{2+} in the $M(1)$, $M(2)$, and $M(3)$ sites. It can be inferred from this discussion and from Burns (1965) that the main band at about 1035 nm arises from Fe^{2+} in the $M(2)$ site. White and Keester (1966) assigned a band in the 2300–2500 nm region to

Fe^{2+} in tetrahedral coordination, also in a spectrum of actinolite. Both of these bands occur in the spectra of the orthorhombic amphiboles of the anthophyllite–gedrite series, $(Mg,Fe,Al)_7(Si,Al)_8O_{22}(OH)_2$; however, Mao and Seifert (1974) assigned both bands to Fe^{2+} in the $M(4)$ site.

The high degree of distortion of the $M(4)$ site is expected to produce large crystal-field splittings analogous to the spectra of Fe^{2+} in the distorted $M(2)$ site of orthopyroxene, $(Mg,Fe)_2Si_2O_6$. Burns (1970), Runciman *et al.*, (1973), and Goldman and Rossman (1976, 1977) studied a variety of orthopyroxenes in which bands at about 930 nm and 1850 nm were assigned to transitions to excited states derived from the splitting of the octahedral ^5E_g state. These interpretations provide a basis for the analysis of the calcic amphibole spectra. A third absorption band at 2350 cm⁻¹ was identified in orthopyroxene (Goldman and Rossman, 1976) and assigned to a transition within the split $^5T_{2g}(O_h)$ state of Fe^{2+} in the $M(2)$ site. We have examined polarized spectra to see if a similar band arising from Fe^{2+} in the $M(4)$ site occurs in the 1200–4000 cm⁻¹ region.

Sample description

Tremolite: Mt. Bity, Malagasy Republic (Lacroix, 1910); CIT #8038; a 2 cm prismatic, euhedral crystal that is green, transparent, and free of inclusions. Microprobe analyses of various chips from the crystal show a range of iron content from 1.6 to 2.8 weight percent FeO, but the microprobe analysis of the

sample used for optical spectra indicated 2.06 percent FeO (Table 1) and the wet chemical analysis of the Mössbauer sample indicated 2.09 percent FeO.

Actinolite: Zillerthal, Tyrol, Austria; CIT #4916; dark green, prismatic, euhedral laths up to 15 mm long and up to 4 mm across the basal section in a talc–mica schist. The absorption spectra were taken in areas on the oriented slabs that were free of micaceous inclusions common to these samples. The microprobe analysis (Table 1) is similar to those reported for actinolites from this locality in Leake (1968).

Pargasite: Pargas, Finland; CIT #2573; large crystal clusters in which the individual crystals are black, tabular along (010), and have other well-developed crystal faces. These crystals occur in marble and commonly have calcite inclusions. The spectra were obtained in inclusion-free areas. The composition of this sample differs from those reported for other pargasites from this locality in Leake (1968) in having higher Fe and lower F and Al.

These minerals did not show chemical zonation in the area in which the optical spectra were taken on the (100) slabs.

Experimental methods

All spectral data presented in this paper have been obtained at room temperature on self-supporting (010) and (100) slabs. The method of preparation and data analysis have been described (Goldman and Rossman, 1977).

The Mössbauer spectrum was obtained at room temperature using a MCA unit driven by a conventional loudspeaker drive system with moving-source geometry. A 16 mc ^{57}Co source in a palladium matrix was used, which produced a minimum line width of 0.27 mm/sec. The velocity increment was approximately 0.04 mm/sec/channel and was calibrated with laboratory standards. The sample concentration was approximately 1 mg Fe/cm^2. The sample was ground under acetone, meshed to obtain a grain size from 43–74 μm and set in lacquer in the bottom of a shallow 1" diameter plastic dish. Nearly 3×10^6 counts per channel were accumulated, and the spectrum was analyzed using the computer program MOSFT (W. A. Dollase, personal communication). Other experimental details are similar to Dollase (1973).

The Mössbauer spectrum of the Mt. Bity tremolite was analyzed for six peaks which included two quadrupole doublets from Fe^{2+} (AA', BB') and one quadrupole doublet from Fe^{3+} (CC'). The half-widths for the two components of each doublet were constrained to be equal, although the half-widths of the different doublets were allowed to vary. Due to the small percentage of Fe^{3+} in this sample, the position of peak C was fixed, the areas of C and C' were constrained to be equal, and their half-widths were specified. The sinusoidal variation of the background was also fitted. The resulting parameters are given in Table 2. A χ^2 value for the 200 channels analyzed is 196.

The electron microprobe analyses (Table 1) of the three amphiboles have been obtained within the areas in which the optical spectra were obtained on the (100) slabs. The analyses of the Mt. Bity and Zillerthal samples were normalized to charge assuming 23

Table 1. Microprobe analyses

SAMPLE	1	2	3
	Weight percent of oxides		
SiO$_2$	57.65	57.01	42.91
TiO$_2$	.07	-	.88
Al$_2$O$_3$	1.31	1.06	12.69
Cr$_2$O$_3$	-	.24	-
MgO	23.62	21.36	14.44
MnO	-	.22	.09
FeO	2.06	5.72	10.25
CaO	13.42	12.30	13.00
Na$_2$O	.61	.41	2.45
K$_2$O	.20	.05	1.57
F	.21	.06	1.66
Cl	.04	-	-
	99.19	98.43	99.94
$-O\equiv F$	.09	.03	.70
$-O\equiv Cl$	.01	-	-
	99.09	98.40	99.24
	Formula Proportions*		
Si	7.81	7.87	6.28
Al(IV)	.19	.13	1.72
Al(VI)	.02	.04	.47
Mg	4.77	4.40	3.15
Ti	.01	-	.10
Cr	- 5.03	.03 5.16	- 4.99
Mn	-	.03	.01
Fe	.23	.66	1.26
Ca	1.95	1.82	2.03
Na	.16	.11	.69
K	.03	.01	.29

1. Tremolite, Mount Bity, Malagasy Republic
2. Actinolite, Zillerthal, Tyrol, Austria
3. Pargasite, Pargas, Finland

*The formula proportions are obtained by normalizing the total positive charge to 46 assuming all Fe is Fe^{2+}.

Table 2. Mössbauer parameters

PEAKS	ISOMER* SHIFT	QUADRUPOLE SPLITTING	HALF-WIDTH	% AREA
AA' Fe^{2+}	1.14	2.82	.32	51.4(±0.92)
BB' Fe^{2+}	1.17	1.84	.34	41.4(±1.22)
CC' Fe^{3+}	0.48	0.74	.53	7.2(±1.20)

*Relative to Fe^0 in mm/sec

oxygens and that all Fe is Fe^{2+}. Mössbauer data presented in this paper for the Mt. Bity sample and the analyses given in Leake (1968) for actinolites from the Zillerthal area indicate that less than 10 percent of the total Fe is Fe^{3+}. Using an Fe^{3+}/Fe ratio of 0.10 does not change these formula proportions. The formula proportions for the Pargas sample have been obtained similarly. Changing the Fe^{3+}/Fe ratio up to 0.30 does not appreciably change the resulting formula proportions. The sum of Al^{VI}, Fe, Mg, Ti, and Mn is close to 5.0, and the sum of Ca, K, and Na is approximately 3.0 with Fe^{3+}/Fe ratios of less than 0.30.

Crystal structure

Calcic amphiboles are monoclinic with space group $C_{2/m}$. The $M(1)$, $M(2)$, and $M(4)$ sites have point-group symmetry C_2, and the $M(3)$ site has point-group symmetry C_{2h}.

The structural differences between the $M(1)$, $M(2)$, and $M(3)$ sites and the $M(4)$ site suggest that the spectroscopic features of ferrous iron in these sites will markedly differ. The (c^*-b) and $(a-c)$ ORTEP (Johnson, 1965) projections of the $M(1)$, $M(2)$, and $M(3)$ sites of actinolite are presented in Figure 1. These sites approach octahedral geometry, with similar average metal–oxygen (M–O) bond distances of 2.105, 2.098, and 2.098 Å, respectively (Mitchell *et al.*, 1971). In comparison, the $M(4)$ site of actinolite shown in Figure 2 is highly distorted and is eight-coordinated when occupied by calcium.

Ideally, absorption spectra would be analyzed using the specific bond angles and bond lengths of a particular metal ion in a coordination polyhedron. For a metal ion in a site that is occupied predominantly by a different metal ion, these structural details are not known, as is the case for Fe^{2+} in the $M(4)$ site of actinolite. The projections of the actinolite $M(4)$ site relate primarily the position of calcium. The C_2 point-group does not constrain Fe^{2+} to occupy the calcium position; the only constraint is that it must, on the average, occupy a position on the two-fold rotation axis parallel to b. The position of Fe^{2+} in the $M(4)$ site of monoclinic amphiboles has been determined in grunerite, $Fe_7Si_8O_{22}(OH)_2$ (Finger, 1969). A comparison of the two sites (Fig. 2) indicates that Fe^{2+} is displaced on the two-fold axis toward the O(2) oxygens relative to the calcium position. An important consequence of this displacement is the increase of the Fe^{2+}–O(5) bond distances to nearly 3.3 Å. For this reason, the grunerite site is considered as a highly distorted, six-coordinate site

(Papike *et al.*, 1969) with the principal distortions being due to (1) an elongation of the Fe^{2+}–O(6) bonds with a reduction in the O(6)–Fe^{2+}–O(6) bond angle; (2) a twisting of the O(6)–O(6) bond about b relative to the O(2)–O(2) bond; (3) a relative compression of the Fe^{2+}–O(4) bonds; and (4) a removal of the center of symmetry. The grunerite $M(4)$ site will be used as the structural model to analyze the bands due to Fe^{2+} in the $M(4)$ site of actinolite. This assumes that Fe^{2+} occupies a "grunerite position" in the actinolite $M(4)$ site.

Description of spectra

The spectra of the Mt. Bity tremolite are presented in Figure 3 to illustrate the features that characterize most calcic amphibole spectra. These spectra will serve as a basis for the identification, assignment, and crystal-field analysis of the absorption bands due to Fe^{2+} in the $M(4)$ site. Many of the features shown in
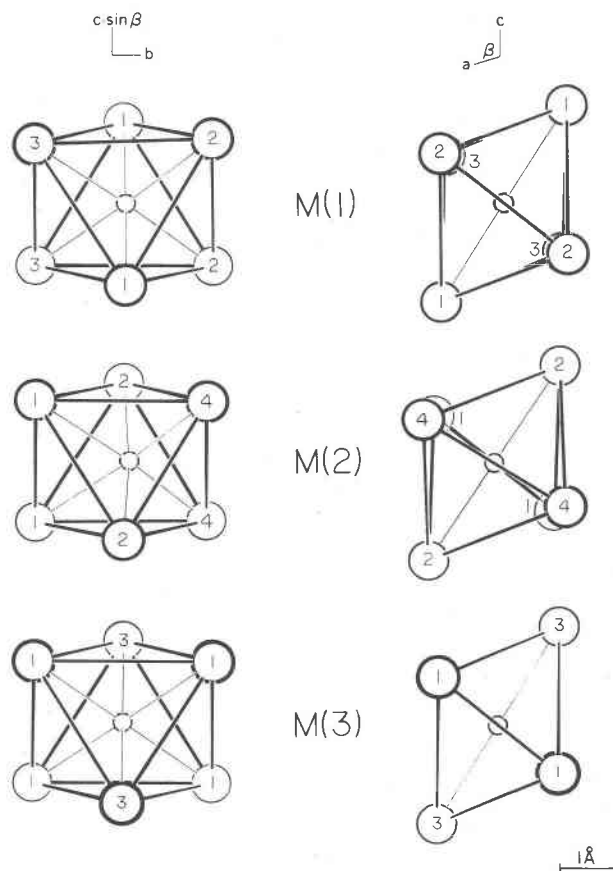

FIG. 1. (c^*-b) and $(a-c)$ ORTEP projections of the $M(1)$, $M(2)$, and $M(3)$ coordination sites in actinolite based on the atomic coordinates given in Mitchell *et al.* (1971). All figures have been drawn to the same scale.
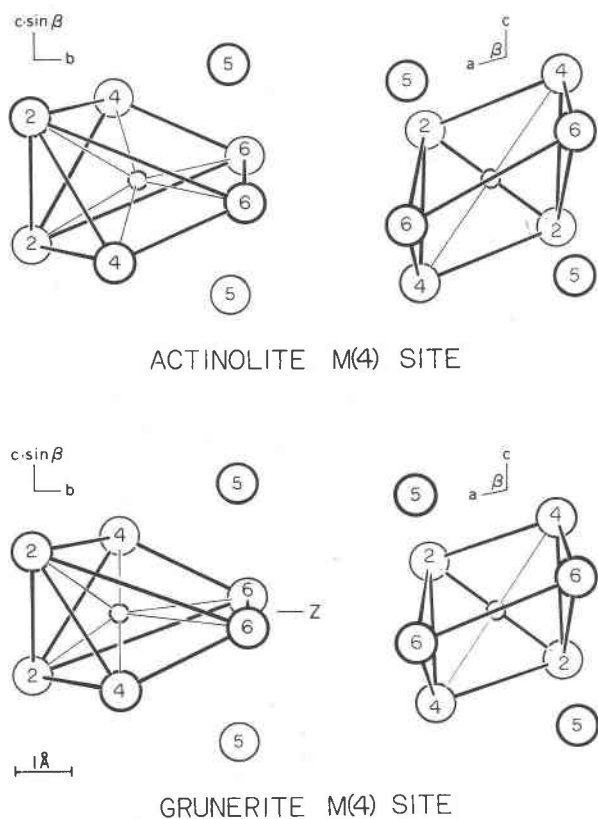
ACTINOLITE M(4) SITE

GRUNERITE M(4) SITE

FIG. 2. (c^*–b) and (a–c) ORTEP projections of the $M(4)$ coordination sites in actinolite and grunerite based on the atomic coordinates given in Mitchell et al. (1971) and Finger (1969), respectively. These projections illustrate the different positioning of iron in the grunerite site from calcium in the actinolite site. All figures are drawn to the same scale.

Figure 3 have been described and assigned in previous studies.

White and Keester (1966) presented an unpolarized spectrum of an actinolite and assigned an absorption band at 1020 nm to Fe^{2+} in six-fold coordination, a sharp band at 1399 nm to the first vibrational overtone of the OH^- stretching mode, and a set of sharp bands at 2320 nm and 2392 nm to infrared combination modes. Burns (1970) presented the spectra of two actinolites and assigned absorption bands at 727 nm in γ and at 661 nm in β to Fe^{2+}/Fe^{3+} intervalence charge-transfer (IVCT) and described four sharp absorption bands in α at about 1400 nm arising from OH^- vibrational overtones. Burns attributed the absorptions in the 800–1300 nm region to Fe^{2+} in the $M(1)$, $M(2)$, and $M(3)$ sites. The band assigned by White and Keester to tetrahedral Fe^{2+} is located in α at approximately 2470 nm (4050 cm^{-1}) in Figure 3. The correct interpretation of this band is

crucial for the site assignment to be discussed in the next section.

In addition to the features discussed in previous investigations, the sharp peaks of low intensity in the 400–550 nm region in Figure 3 are identified as spin-forbidden, electronic transitions of Fe^{2+} and Fe^{3+}. Sharp bands at 2297 nm and 2384 nm in β and at 2315 nm and 2387 nm in γ correspond to the locations of the combination bands described by White and Keester.

Fe^{2+} in $M(4)$

The prominent absorption bands at 1030 nm in β and at 2470 in α are assigned to transitions of Fe^{2+} in the $M(4)$ site. The evidence supporting this assignment is derived from (1) the similarity to the spectra of Fe^{2+} in the $M(4)$ sites of the Mg–Fe amphiboles and in the $M(2)$ sites of ortho- and clinopyroxene, (2) the intensity correlation between these bands, (3) the barycenter energy of the two bands, and (4) the intensity of the 1030 nm band.

Similarity of spectra

The locations of the 1030 nm and 2470 nm bands are similar to those reported for other large, distorted sites. The spectra of Fe^{2+} in the $M(4)$ sites of cummingtonite–grunerites (Burns, 1970) show a dominant absorption band in the 1000 nm region. In the spectra of anthophyllite and gedrite, Mao and Seifert (1973) assigned bands near 1000 nm and 2500 nm to Fe^{2+} in the $M(4)$ site. Fe^{2+} in the distorted $M(2)$ sites of orthopyroxene (Burns, 1970; Runciman et al., 1973; Goldman and Rossman, 1976, 1977) and clinopyroxene (Bell and Mao, 1972; Burns et al., 1972) also have bands in the 1000 nm and 1800–2500 nm regions. Therefore, it is apparent that these large, distorted sites produce a crystal-field splitting of about 5500 cm^{-1} which results in one band in the 1000 nm region and the other in the 2000 nm region. Absorption bands due to Fe^{2+} in the smaller pyroxene $M(1)$ sites do not occur above 1200 nm. If it can be shown that these two bands arise from the same Fe^{2+} ion, then these observations support an $M(4)$ site origin for the two calcic amphibole bands and exclude their origin from the $M(1)$, $M(2)$, and $M(3)$ sites.

Band correlations

Sections of the Mt. Bity tremolite were heated in air at 535°C for 8 hours. After the sample was heated, the 1030 nm band in β retained only 50 percent of its unheated intensity (Figure 4). A similar value is ob-
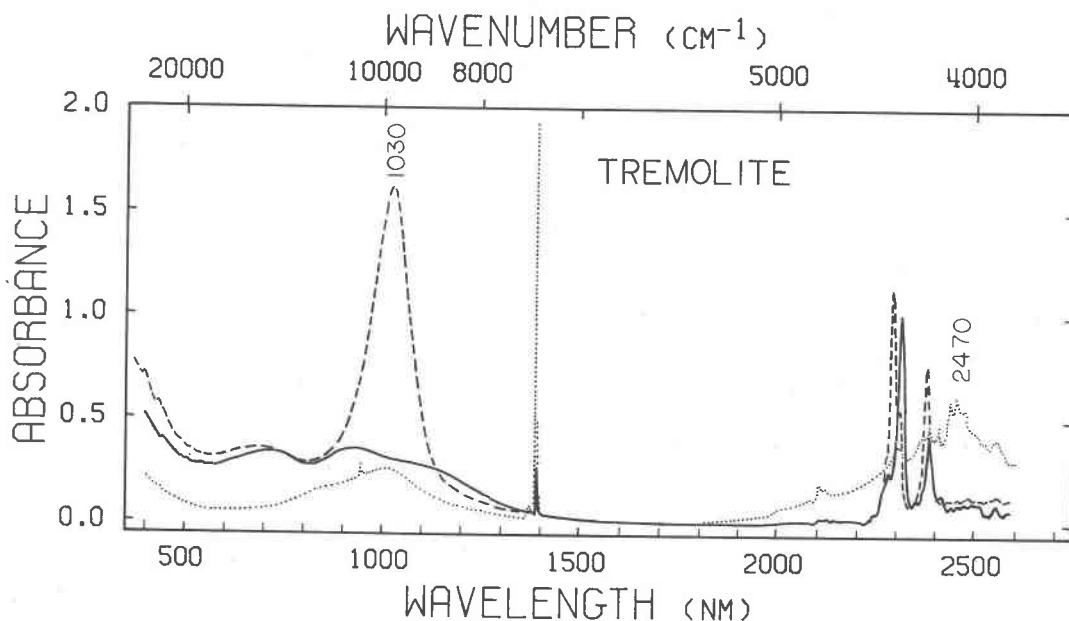
FIG. 3. Room temperature spectra of tremolite from Mt. Bity, Malagasy Republic. α spectrum (. . . .), β spectrum (-------), and γ spectrum (———). $\alpha \wedge c = 17°$. Crystal thickness = 1.0 mm.

tained for the 2470 nm band, although the vibrational absorptions superimposed upon this band preclude an exact determination of the reduction factor. These data suggest that both the 1030 nm and 2470 nm bands arise from the same Fe^{2+} ion.

The spectra of two additional calcic amphiboles have been obtained to verify that both bands originate from the same Fe^{2+} ion. Spectra of an actinolite are presented in Figure 5 in which the 1030 and 2470 nm bands are approximately 3.1 times as intense as the analogous bands in Figure 3. Stoichiometry considerations for this sample (Table 2) indicate that there is an excess of Al^{VI}, Mg, Cr, Mn, and Fe that cannot be accommodated in the five $M(1)$, $M(2)$, and $M(3)$ sites in the half-unit cell. Hence, the excess must be accommodated in $M(4)$, which has only 1.82 of 2.0 possible sites occupied by Ca. In addition, there is not enough Ca and Na to completely fill the $M(4)$ site. Furthermore, the spectra of pargasite, $NaCa_2(Mg,Fe^{2+})_4(Al,Fe^{3+})Si_6Al_2O_{22}(OH,F,Cl)_2$, (Fig. 6) indicate that the absence of the 1030 nm band is correlated with the absence of the 2470 nm band. Regardless of the Fe^{3+}/Fe^{2+} ratio assumed for this sample, the resulting formulas from the microprobe analysis indicate that the $M(4)$ site is fully occupied by Ca and that the sum of the remaining octahedral cations is approximately 5.0. In summary, these spectra indicate that both absorption bands are either simultaneously present or absent, and hence, they must arise from the same Fe^{2+} ion.

Barycenter energy

The $M(2)$ Fe^{2+} absorption bands at about 930 nm and 1850 nm in orthopyroxene are derived from the splitting of the $^5E_g(O_h)$ state due to the low symmetry of this site. Based upon the interpretation of Runciman *et al.*, Mao and Seifert concluded that the similar bands in anthophyllite and gedrite were due to the splitting of this state. The results of a study by Faye (1972) support these interpretations, and hence, support the assignment of the 1030 nm and 2470 nm bands as electronic transitions to the separated $^5E_g(O_h)$ components of Fe^{2+} in the $M(4)$ site. Faye correlated the barycenter energy of the two components with the average M–O bond length of six-coordinate sites in a variety of minerals. While slightly modifying the average M–O bond distance to account for the effect of the substitution of other metal ions into each site, it was found that the barycenter energy decreased linearly with increasing average M–O bond length. Using the average for the six M–O bond lengths in the grunerite $M(4)$ site of 2.29 Å (Finger, 1969), a barycenter energy of 6880 cm^{-1} is predicted from Faye's correlation. This is the same value that is obtained from the tremolite spectra in Figure 3. For comparison, the smaller $M(2)$ site in
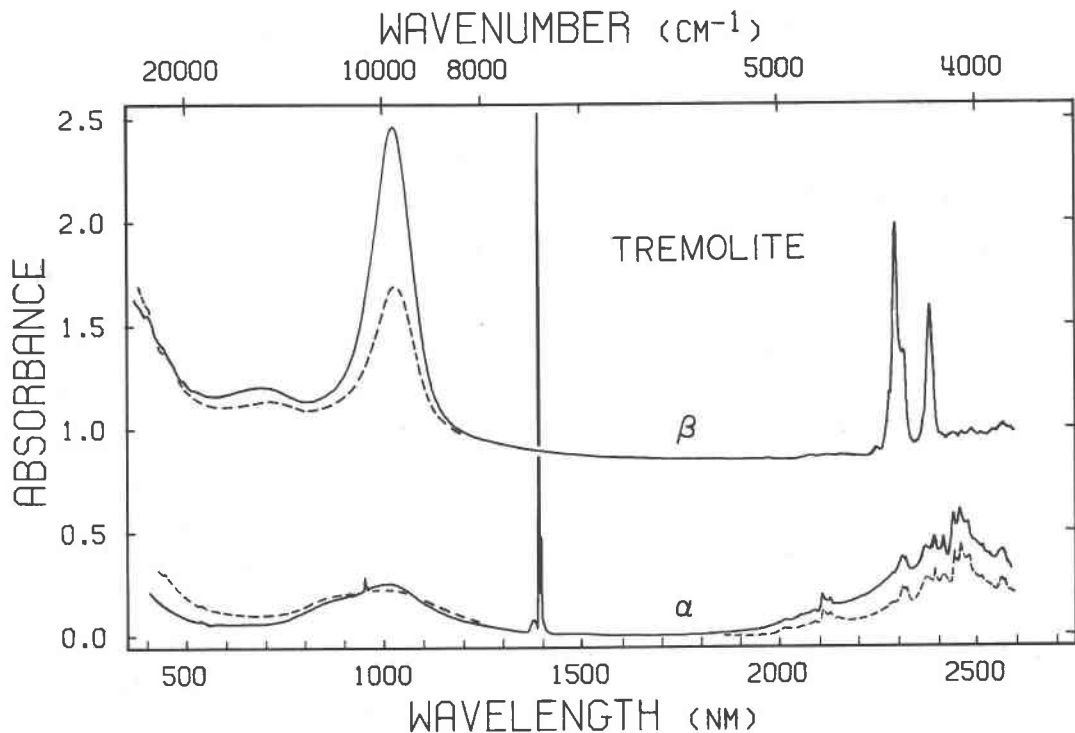
FIG. 4. Spectra tremolite from Mt. Bity, Malagasy Republic, before heating (———) and after heating in air at 535°C for 8 hours (-------). The bands at 1030 nm in β and 2470 nm in α are reduced to nearly half of their original intensity after heating which suggests a common Fe^{2+} origin. Crystal thickness = 1.0 mm. The β-spectra have been displaced vertically for clarity.

the orthopyroxene bronzite, having an average M–O bond distance of 2.22 Å, has a barycenter energy of about 8160 cm^{-1}. In addition, Faye's correlation argues against the possibility that the 2470 nm band, and hence, the 1030 nm band, arise from Fe^{2+} in the $M(1)$, $M(2)$, or $M(3)$ sites. The predicted barycenter energies of absorption bands arising from these sites, having average M–O bond lengths of about 2.1 Å, are about 10,000 cm^{-1}, which precludes the occurrence of one component at 2500 nm (4000 cm^{-1}). The remaining Fe^{2+} bands in the near-infrared region occur between 850 nm and 1150 nm. Taking these limits as the maximum extent of the ^5E_g splitting for Fe^{2+} in the $M(1)$, $M(2)$, or $M(3)$ sites, a barycenter energy of 10,200 cm^{-1} is obtained. The agreement with Faye's correlation supports their assignment to Fe^{2+} in the $M(1)$, $M(2)$, or $M(3)$ sites. It is concluded that both the 1030 nm and the 2470 nm absorption bands in the spectra of calcic amphiboles arise from Fe^{2+} in the $M(4)$ site and that these bands result from the splitting of the $^5E_g(O_h)$ state in the low-symmetry environment.

Intensity considerations

The intensification of absorption features in distorted sites lacking centers of symmetry is a well-known phenomenon (Burns, 1970; White and Keester, 1967). The greater intensity of the 1030 nm band in β, in comparison with other Fe^{2+} features in the 800–1300 nm region, provides an indication that this band is due to Fe^{2+} in a non-centrosymmetric site. Although the $M(1)$ and $M(2)$ sites lack centers of symmetry, they are not nearly as distorted or non-centrosymmetric as the $M(4)$ site. Therefore Fe^{2+} in the $M(4)$ site is the most likely candidate for the 1030 nm band. This assignment, indicated by the band positions, can be evaluated by comparing the absolute intensity of the 1030 nm band (expressed in terms of molar absorptivity, ϵ_{1030}) with ϵ values from sites of various coordination geometries. Although an accurate value for ϵ_{1030} cannot be determined because the Fe^{2+} contents of various sites are not known, electron microprobe and Mössbauer analyses of the Mt. Bity tremolite provide constraints to derive a lower limit.
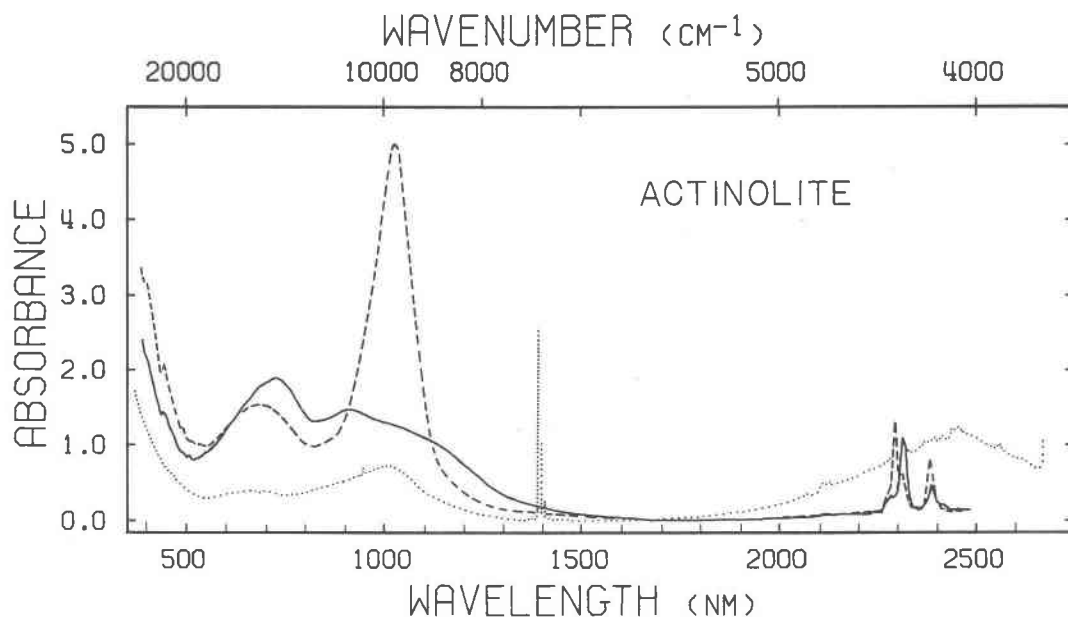
FIG. 5. Room temperature spectra of actinolite from Zillerthal, Tyrol, Austria. α spectrum (. . . . .), β spectrum (------), and γ spectrum (———). $\gamma \wedge c = 16°$. Crystal thickness = 1.0 mm.

An absolute lower limit for ϵ_{1030} of 16 is obtained from the formula, assuming all iron is Fe^{2+} and that all of it contributes to the band. However, the presence of Fe^{2+}/Fe^{3+} IVCT bands in γ and β in the 600–750 nm region, as well as aspects of the Mössbauer spectrum (below) indicate that some iron is Fe^{3+}. If the 1030 nm band is due to Fe^{2+} in $M(4)$, the presence of Fe^{3+} in this sample is suggested in the +0.5 mm/sec region, although a distinct peak is not observed.
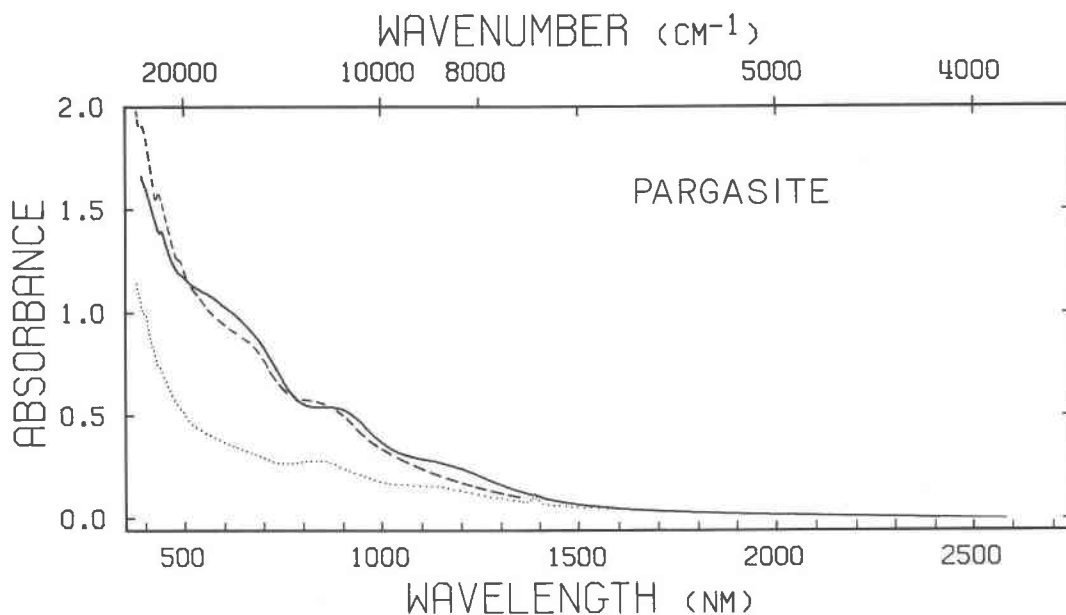

FIG. 6. Room temperature spectra of pargasite from Pargas, Finland. α spectrum (. . . . .), β spectrum (-------), and γ spectrum (———). $\gamma \wedge c = 24°$. Crystal thickness = 0.10 mm.

The Mössbauer data for the Mt. Bity tremolite provide further constraints on the lower limit of ϵ_{1030}. The room temperature Mössbauer spectrum of this sample (Fig. 7) shows two distinct peaks in the high-velocity region (2.0–2.5 mm/sec) that are attributable to Fe^{2+} in at least two distinct environments. The presence of Fe^{3+} in this sample is suggested in the + 0.5 mm/sec region, although a distinct peak is not observed.

The Mössbauer studies of the calcic amphiboles by Bancroft *et al.* (1967c), Häggström *et al.* (1969), Burns and Greaves (1971), and Bancroft and Brown (1975) have assumed that Ca, Na, and K completely fill the $M(4)$ site, and hence, peak assignments have been made only for Fe^{2+} in the $M(1)$, $M(2)$, and $M(3)$ sites, with the peaks having the smallest quadrupole splitting assigned to Fe^{2+} in the $M(2)$ site. Fe^{2+} in the $M(4)$ site has been identified in the Mössbauer spectra of cummingtonites and grunerites (Bancroft

et al., 1967b; Hafner and Ghose, 1971). These spectra are characterized by two distinct quadrupole doublets: the outer doublet has a quadrupole splitting of about 2.7–2.8 mm/sec and is assigned to Fe^{2+} in the $M(1)$, $M(2)$, and $M(3)$ sites; the inner doublet has a quadrupole splitting of 1.5–1.8 mm/sec and is assigned to Fe^{2+} in the $M(4)$ site.

Making the reasonable assumption that the band at 1030 nm is due to Fe^{2+} in one site only, the existence of two doublets in the spectrum of Mt. Bity tremolite establishes that ϵ_{1030} must be greater than 16, *i.e.* at least 27 if the band is due to the site giving rise to peaks AA', and at least 40 if it is due to the site giving rise to BB'. If the Mössbauer peaks in question represent more than one site, the value of ϵ_{1030} could only be higher.

Thus, if we assign AA' to $M(1)$ and $M(3)$, and BB' to $M(2)$ in accordance with previous work on calcic amphiboles, we obtain minimum values of ϵ_{1030} equal
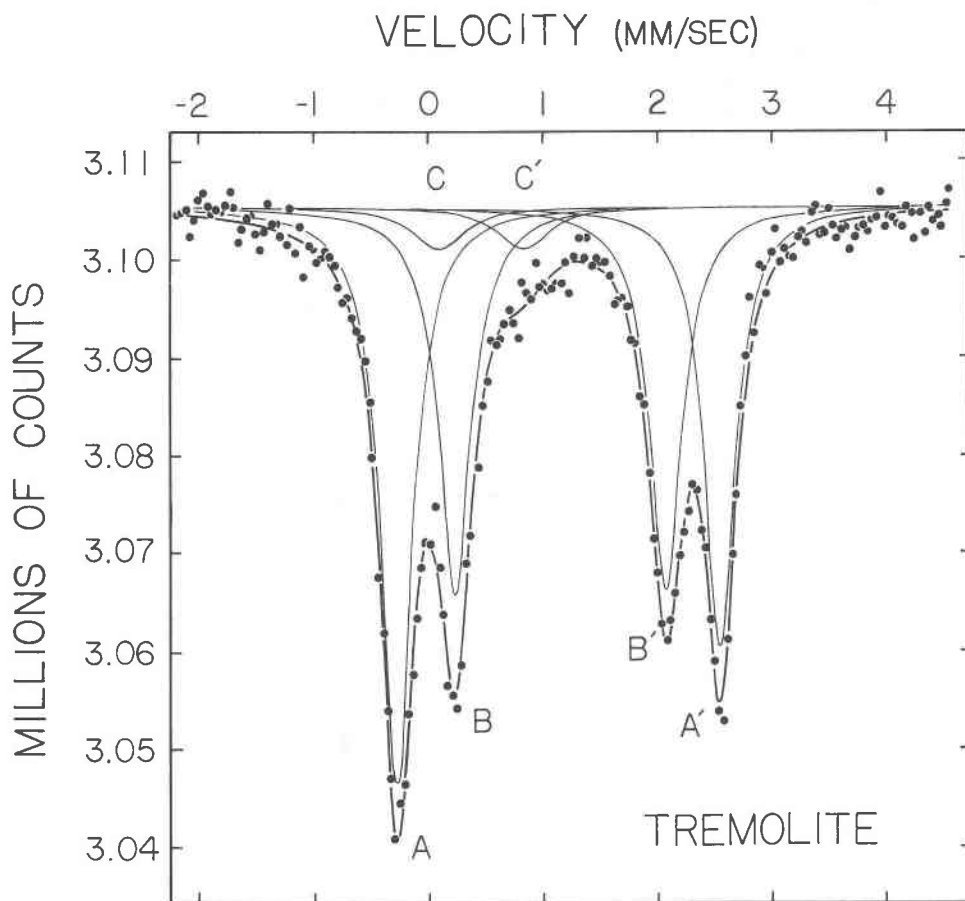
VELOCITY (MM/SEC)

FIG. 7. Mössbauer spectrum of tremolite, Mt. Bity, Malagasy Republic, taken at room temperature. The spectrum is presented relative to Fe^0.

to (1) 40 if the band is due to $M(2)$; (2) 27 if it is due to $M(1)$ or $M(3)$, and (3) very large (well over 40) if it is due to $M(4)$. If we assign peaks BB' to $M(4)$ and AA' to $M(1)$, $M(2)$, and $M(3)$, we obtain minimum values for ϵ_{1030} of (1) 40 if the band is due to $M(4)$, and (b) 27 if it is due to $M(1)$, $M(2)$, or $M(3)$.

The ϵ values for Fe^{2+} absorption bands in other sites (Table 3) can be compared with the lower limit determined for ϵ_{1030}. The smaller sites such as the $M(1)$ sites in olivine and orthopyroxene have ϵ values of less than 10, even though these sites have different distortions and departures from centrosymmetry. The larger sites in the pyroxenes and amphiboles have larger ϵ values. Based on this comparison, an ϵ value for the 1030 nm band of greater than 27 is consistent with an assignment to Fe^{2+} in the $M(4)$ site, but probably inconsistent with assignment to any other site.

Other considerations

Due to similar types of distortions of the calcic amphibole $M(4)$ site and the orthopyroxene $M(2)$ site involving elongation of two adjacent M–O bonds, and due to the similar crystal-field splittings of the $^5E_g(O_h)$ state for these minerals, the spectra of the Mt. Bity tremolite were obtained in the 1200–4200 cm^{-1} region (Fig. 8) to search for a low-energy absorption band analogous to the 2350 cm^{-1} band in orthopyroxene. The absorption bands in the 3600–3750 cm^{-1} region arise from OH$^-$ stretching motions, and the absorptions below 2000 cm^{-1} also

have a vibrational origin. Another band due to $M(4)$ Fe^{2+} does not occur in this region above 2000 cm^{-1}.

Both the 1030 nm band in β and the 2470 band in α in the spectra of pargasite are absent. The absorption band in α at 1030 nm is also absent in Figure 6, although it is present in both the tremolite and actinolite spectra. Furthermore, this band was reduced in intensity in the heat-treated tremolite spectra. To examine the possibility that this band may be due to Fe^{2+} in the $M(4)$ site, the intensities for the α and β bands at 1030 nm were compared for fourteen calcic amphibole samples (Fig. 9). The trend of these data suggests that the α and β bands are correlated. Consequently, the absorption band at 1030 nm in α is assigned to $M(4)$ Fe^{2+}. The possibility that the α band results from the mixing of intensities from the intense β peak due to experimental problems does not appear likely, because there is little evidence for mixing of polarization intensities in the 2000–2500 nm region.

Crystal-field analysis

The crystallographic point-group symmetry of the calcic amphibole $M(4)$ site is C_2 with the two-fold rotation axis parallel to b which bisects the O(6)–$M(4)$–O(6) and O(2)–$M(4)$–O(2) bond angles. For spectroscopic analysis, the Z crystal-field axis is taken along b to coincide with the axis of highest symmetry of the site. The relative ordering of the crystal-field states and the polarization properties of the allowed transitions for C_2, in which Z is a dihe-

TABLE 3. ϵ values for common minerals

MINERAL	SITE	BAND (cm^{-1})	ϵ (ℓ/mole cm)	REFERENCE*
OLIVINE (FAYALITE)	M(1)	10,930	2.4	(1),{1},[2],[3]
	M(2)	9,290	8.6	
ORTHOPYROXENE (BRONZITE)	M(2)	10,930	41	(4),{4},[5]
ORTHOPYROXENE (ORTHOFERROSILITE)	M(1)	8,560	∼10	(1),{6},[5]
Mg-Fe AMPHIBOLE (GEDRITE)	M(4)	∼10,600	∼20	(7),{8},[8]
Mg-Fe AMPHIBOLE (GRUNERITE)	M(4)	9,980	∼80	(1),{9},[9]
GARNET (PYROPE-ALMANDINE)	8-fold	7,830	1.1	(10),{10}
CORDIERITE	6-fold	8,200	4	(11),{11},[11]

1. Burns (1970)
2. Bush et al. (1970)
3. Birle et al. (1968)
4. Goldman and Rossman (1976b)
5. Bancroft, Burns and Howie (1967)
6. Kuno (1954)
7. Mao and Seifert (1974)
8. Papike and Ross (1970)
9. Bancroft, Burns and Maddock (1967)
10. White and Moore (1972)
11. Goldman and Rossman (in preparation)

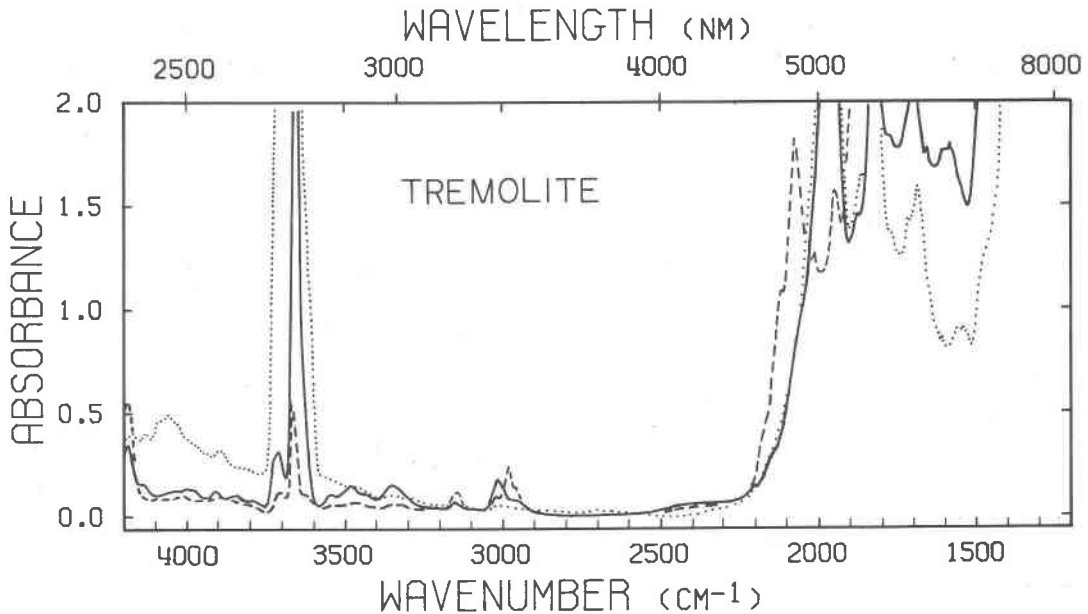* ( ) = Spectral Data   [ ] = Site Population Data   { } = Chemical Data

FIG. 8. Room temperature, mid-infrared spectra of tremolite from Mt. Bity, Malagasy Republic, showing that a second M(4) Fe^{2+} absorption band does not occur in this region above 2000 cm^{-1}. α spectrum (. . . .), β spectrum (-------), and γ spectrum (———). $\gamma \wedge c = 17°$. Crystal thickness = 1.0 mm.

dral axis, are presented in Figure 10. The classification of states is derived from the "descent in symmetry" method from O_h to D_{4h} to $C_{2v}(C_2'')$ to $C_2(C_2'')$ using the correlation tables in Wilson et al. (1955), and the polarization properties of the allowed transitions are obtained from the character table for C_2 in Cotton (1963). Tetragonal compression between O_h and D_{4h} and acute dihedral angles about Z are used based on the structural data. The upper two states and the lower three states are derived from the octahedral ^5E_g and $^5T_{2g}$ states of Fe^{2+}, respectively. Although C_2 explains the polarization of the 1030 nm band mostly in $Z(\beta)$, it cannot explain the complete polarization of the 2470 nm band in α. This transition is expected to occur in both $\alpha(X)$ and $\gamma(Y)$. Therefore, the polarization properties of these bands are indicative of a higher, effective electrostatic symmetry.
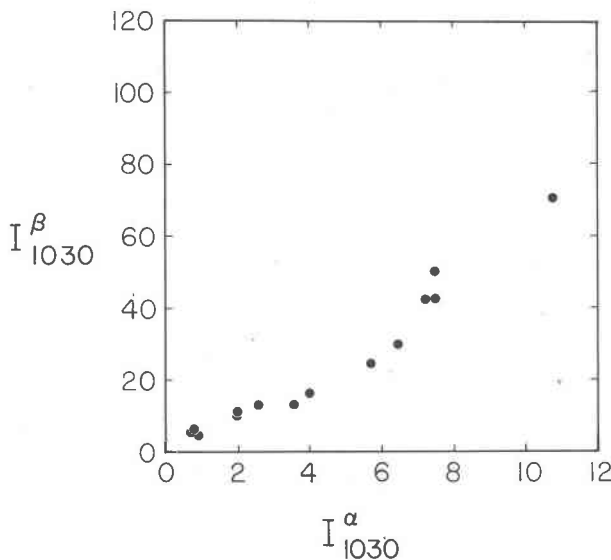
The effective electrostatic symmetry of the calcic amphibole $M(4)$ site is taken to be $C_{4v}(C_2'')$, based upon the similar interpretation of the analogous bands in the spectra of orthopyroxene by Runciman et al., and Goldman and Rossman (1977), and anthophyllite and gedrite by Mao and Seifert. From the classification of states and the allowed transitions for C_{2v}, the 1030 nm and 2470 nm absorption bands are assigned to the $A_1 \rightarrow A_1$ and $A_1 \rightarrow B_1$ transitions, respectively. The $A_1 \rightarrow B_2$ transition within the split $^5T_{2g}(O_h)$ state, which was identified at 2350 cm^{-1} in the spectra of orthopyroxene, does not occur at energies greater than 2000 cm^{-1}. For C_{2v} symmetry, this transition is expected to be polarized in $\gamma(Y)$ as shown in Figure 10.

FIG. 9. Intensity correlation of the calcic amphibole absorption bands in β and α at 1030 nm suggesting that the α band is also due to Fe^{2+} in the $M(4)$ site. All points represent room temperature spectra normalized to 1.0 cm thickness.

The operator-equivalent method described by Hutchings (1964) to derive energy expressions for the crystal-field states was used by Goldman and Rossman (1977) to analyze the spectra of Fe^{2+} in the $M(2)$ site of orthopyroxene. In orthopyroxene, all three allowed transitions of C_{2v} were observed experimentally, and hence the three crystal-field fitting parameters were calculated; $\Delta(= 10\ D_q)$, M, and N. From these parameters, the energy of the forbidden $A_1 \rightarrow A_2$ transition was calculated. However, the energy of the $A_1 \rightarrow B_2$ transition due to Fe^{2+} in the $M(4)$ site of calcic amphiboles is not known, although the mid-infrared spectra of the Mt. Bity tremolite indicate that it does not occur above 2000 cm^{-1}. Using this value as an upper limit for the $A_1 \rightarrow B_2$ transition, the following results are obtained: $\Delta = 4629$ cm^{-1} and $A_1 \rightarrow A_2 = 976$ cm^{-1}. If $A_1 \rightarrow B_2$ occurs at 1400 cm^{-1}, the crystal-field parameters change as follows: $\Delta = 4760$ cm^{-1}, and $A_1 \rightarrow A_2 = 524$ cm^{-1}.

The value determined for Δ, the energy separation between the octahedral $^5T_{2g}$ and ^5E_g states in the 4600–4800 cm^{-1} range has been obtained from the point-charge model in which the crystal-field potential was derived in terms of the average $M-O$ bond distance of the $M(4)$ site. Although a Δ of this magnitude for a six-coordinate site at first seems low, its value is acceptable upon considering orthopyroxene spectral data. The $A_1 \rightarrow A_1$, $A_1 \rightarrow B_1$ and $A_1 \rightarrow B_2$ transitions of bronzite occur at 10,930 cm^{-1}, 5400 cm^{-1}, and 2350 cm^{-1}, respectively. Using the average $M-O$ bond distance of the $M(2)$ site of 2.22 Å, Δ was calculated to be 6522 cm^{-1}. In comparison, the smaller Δ value for $M(4)$ Fe^{2+} in calcic amphiboles reflects the larger size of the $M(4)$ site as expected from the $1/r^5$ dependence of Δ. The energies of the transitions to the A_1 and B_1 states are about 1000 cm^{-1} and 1400 cm^{-1} smaller than the energies of the analogous transitions in orthopyroxene, respectively. This indicates that the energy of the $E_g(O_h)$ state, from which A_1 and B_1 are derived, is also at least 1000 cm^{-1} lower in the calcic amphibole $M(4)$ site, and hence Δ is expected to be reduced from the orthopyroxene value by about this magnitude. Therefore, a Δ for $M(4)$ Fe^{2+} in the 4600–4900 cm^{-1} range is reasonable.

Goldman and Rossman (1977) indicated that the O–M–O bond angles about the crystal-field Z axis play a significant role in determining the energy of the $A_1 \rightarrow B_2$ transition within the split $^5T_{2g}(O_h)$ state. The O(6)–$M(4)$–O(6) angle of 62° is 10° smaller than the O(6)–$M(2)$–O(3) angle in orthopyroxene. The smaller angle about Z is expected to raise the energy
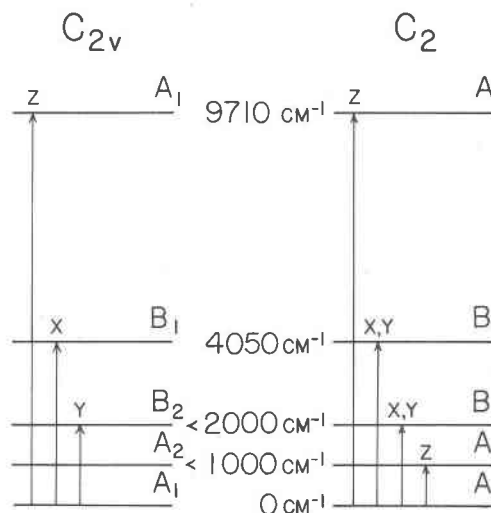

FIG. 10. Energy level schemes for C_2 and C_{2v} symmetries in which the crystal-field Z axis is a dihedral axis. The C_{2v} energy level scheme explains the polarization properties of the $M(4)$ Fe^{2+} absorption bands. C_2, the crystallographic point-group symmetry of the $M(4)$ site, cannot explain the polarization of the 2470 nm band in α.

of the $A_1 \rightarrow B_2$ transition. However, the two elongated $M-O$ bonds in orthopyroxene are about 2.5 Å, whereas they are nearly 2.8 Å in grunerite. This longer bond distance explains the lower energy of $A_1 \rightarrow B_2$ transition in the amphibole $M(4)$ site.

Finally, it was suggested that Fe^{2+} in the $M(4)$ site also produces a band in α at 1030 nm. Since $A_1 \rightarrow A_1$ is expected to be polarized entirely in β, the presence of the α band at 1030 nm is difficult to explain. Similarly, in the spectra of $M(2)$ Fe^{2+} in orthopyroxene, the polarization intensities of the subsidiary components of the main bands were not accounted for using the most intuitively reasonable selection for the C_{2v} axes, although the polarization intensities of the main bands were correctly explained. It must be remembered that these results are based upon a theoretical treatment that is highly idealized, both with regard to the presumed effective symmetry and the assumption of equivalent point-charge contributions from each of the ligands. Nevertheless, on a comparative level, the crystal-field analysis of the calcic amphibole and orthopyroxene spectral data produce consistent results.

Conclusion

The electronic absorptions arising from ferrous iron in the $M(4)$ site of calcic amphiboles have been identified. The absorption bands due to $M(4)$ Fe^{2+}

occur at 1030 nm in β, with some intensity in α, and at 2470 nm in α. The spectra of a wide variety of calcic amphiboles indicate that the Fe^{2+} content in the $M(4)$ site is variable. In particular, $M(4)$ Fe^{2+} has been found in absorption spectra of all actinolite samples studied in this laboratory. The indication from the absorption spectra that the $M(4)$ Fe^{2+} content exhibits significant variation may be important petrologically, due to the temperature and pressure dependencies of the various elemental partitions that involve iron, either between coexisting minerals, or among the crystallographically distinct sites within each mineral.

Acknowledgments

References

Bancroft, G. M. and J. R. Brown (1975) A Mössbauer study of coexisting hornblendes and biotites: Quantitative Fe^{3+}/Fe^{2+} ratios. *Am. Mineral.*, 60, 265–272.

——, R. G. Burns and R. A. Howie (1967a) Determination of the cation distribution in the orthopyroxene series by the Mössbauer effect. *Nature*, 213, 1221–1223.

——, —— and A. G. Maddock (1967b) Determination of cation distribution in the cummingtonite–grunerite series by Mössbauer spectra. *Am. Mineral.*, 52, 1009–1026.

——, A. G. Maddock and R. G. Burns (1967c) Applications of the Mössbauer effect to silicate mineralogy. Part I. Iron silicates of known crystal structure. *Geochim. Cosmochim. Acta*, 31, 2219–2246.

Bell, P. M. and H. K. Mao (1972) Crystal-field effects of iron and titanium in selected grains of Apollo 12, 14, and 15 rocks, glasses, and fine fractions. *Proc. Third Lunar Sci. Conf., Geochim. Cosmochim. Acta, Suppl. 3, Vol. 1,* 545–553.

Birle, J. D., G. V. Gibbs, P. B. Moore and J. V. Smith (1968) Crystal structures of natural olivines. *Am. Mineral.*, 53, 807–824.

Burns, R. G. (1965) *Electronic spectra of silicate minerals: applications of crystal field theory to aspects of geochemistry.* Ph.D. thesis, University of California, Berkeley, California.

—— (1970) *Mineralogical Applications of Crystal Field Theory*, Cambridge University Press. Cambridge, England.

——, R. M. Abu-Eid and F. E. Huggins (1972) Crystal field spectra of lunar pyroxenes. *Proc. Third Lunar Sci. Conf., Geochim. Cosmochim. Acta, Suppl. 3, Vol. 1,* 533–543.

—— and C. Greaves (1971) Correlations of infrared and Mössbauer site population measurements of actinolites. *Am. Mineral.* 56, 2010–2033.

Bush, W. R., S. S. Hafner and D. Virgo (1970) Some ordering of iron and magnesium at the octahedrally coordinated sites in a magnesium-rich olivine. *Nature*, 227, 1339–1341.

Cotton, F. A. (1963) *Chemical Applications of Group Theory*. Wiley-Interscience, New York.

Dollase, W. A. (1973) Mössbauer spectra and iron distribution in the epidote-group minerals. *Z. Kristallogr.*, 138, 41–63.

Faye, G. H. (1972) Relationship between crystal-field splitting parameter, "Δ_{VI}," and M_{host}–O bond distance as an aid in the interpretation of absorption spectra of Fe^{2+} materials. *Can. Mineral.*, 11, 473–487.

Finger, L. W. (1969) The crystal structure and cation distribution of a grunerite. *Mineral. Soc. Spec. Pap. No. 2*, 95–100.

Goldman, D. S. and G. R. Rossman (1976) Identification of a mid-infrared electronic absorption band of Fe^{2+} in the distorted $M(2)$ site of orthopyroxene, $(Mg,Fe)SiO_3$. *J. Chem. Phys. Lett.*, 41, 474–475.

—— and —— (1977) The spectra of iron in orthopyroxene revisited the splitting of the ground state. *Am. Mineral.*, 62, 151–157.

Hafner, S. S. and S. Ghose (1971) Iron and magnesium distribution in cummingtonites $(Fe,Mg)_7Si_8O_{22}(OH)_2$. *Z. Kristallogr.*, 133, 361–376.

Häggström, L., R. Wappling and H. Annersten (1969) Mössbauer study of oxidized iron silicate minerals, *Phys. Stat. Solidi*, 33, 741–748.

Hutchings, M. T. (1964) Point-charge calculations of energy levels of magnetic ions in crystalline electric fields. *Solid State Phys.*, 16, 227–273.

Johnson, C. K. (1965) ORTEP, a FORTRAN thermal ellipsoid plot program for crystal structure illustrations. *U. S. Natl. Tech. Inf. Serv.* ORNL-3794.

Kuno, H. (1954) Study of orthopyroxenes from volcanic rocks. *Am. Mineral.*, 39, 30–46.

Lacroix, A. (1910) *Mineralogie de la France et de ses Colonies. Tome IV*, p. 786.

Leake, B. E. (1968) A catalog of analyzed calciferous and sub-calciferous amphiboles together with their nomenclature and associated minerals. *Geol. Soc. Am. Spec. Pap. No. 98*.

Mao, H. K. and F. Seifert (1974) A study of crystal-field effects of iron in the amphiboles anthophyllite and gedrite. *Carnegie Inst. Wash. Year Book*, 73, 500–503.

Mitchell, J. T., F. D. Bloss and G. V. Gibbs (1971) Examination of the actinolite structure and four other $C_{2/m}$ amphiboles in terms of double bonding. *Z. Kristallogr.*, 133, 273–300.

Papike, J. J. and M. Ross (1970) Gedrite: crystal structures and intracrystalline cation distributions. *Am. Mineral.*, 55, 304–305.

——, —— and J. R. Clark (1969) Crystal-chemical characterization of clinoamphiboles based on five new structure refinements. *Min. Soc. Am. Spec. Pap. No. 2*, 117–136.

Runciman, W. A., D. Sengupta and M. Marshall (1973) The polarized spectra of iron in silicates. I. Enstatite. *Am. Mineral.*, 58, 444–450.

White, W. B. and K. L. Keester (1966) Optical absorption spectra of iron in the rock-forming silicates. *Am. Mineral.*, 51, 774–791.

—— and —— (1967) Selection rules and assignments for the spectra of ferrous iron in pyroxenes. *Am. Mineral.*, 52, 1508–1514.

—— and R. K. Moore (1972) Interpretation of the spin-allowed bands of Fe^{2+} in silicate garnets. *Am. Mineral.*, 57, 1692–1710.

Wilson, E. B., J. C. Decius and P. C. Cross (1955) *Molecular Vibrations*. McGraw-Hill, New York.